Identification of specific histidines as pH sensors in flavivirus membrane fusion

Richard Fritz, Karin Stiasny, and Franz X. Heinz

Institute of Virology, Medical University of Vienna, 1095 Vienna, Austria

The flavivirus membrane fusion machinery, like that of many other enveloped viruses, is triggered by the acidic pH in endosomes after virus uptake by receptor-mediated endocytosis. It has been hypothesized that conserved histidines in the class II fusion protein E of these viruses function as molecular switches and, by their protonation, control the fusion process. Using the mutational analysis of recombinant subviral particles of tick-borne encephalitis virus, we provide direct experimental evidence that the initiation of fusion is crucially dependent on the protonation of one of the conserved histidines (His323) at the interface between domains I and III of E, leading to the dissolution of domain interactions and to the exposure of the fusion peptide. Conserved histidines located outside this critical interface were found to be completely dispensable for triggering fusion.

Introduction

The entry of enveloped viruses into host cells involves a fusion step between the viral and a cellular membrane. This process is mediated by viral fusion proteins that are associated with the viral membrane and primed to undergo structural rearrangements that drive fusion (Kielian and Rey, 2006; Weissenhorn et al., 2007; Harrison, 2008; White et al., 2008). These conformational changes are activated by specific triggers, allowing fusion to occur at the right time and at the right place in the viral life cycle. Different trigger mechanisms (and combinations thereof) have been identified, including (a) interactions with cellular receptors, leading to fusion at the plasma membrane, and (b) protonation by the acidic pH in endosomes, leading to fusion from within endosomes after virus uptake by receptor-mediated endocytosis (White et al., 2008). In the latter case, like in other protein systems of intracellular pH sensors (Srivastava et al., 2007), histidines have been discussed to play a key role as molecular switches because their protonation state changes from uncharged to doubly positively charged at the slightly acidic pH found in endosomes (Carneiro et al., 2003; Bressanelli et al., 2004; Stevens et al., 2004; Kampmann et al., 2006; Kanai et al., 2006; Roussel et al., 2006; Mueller et al., 2008; Roche et al., 2008; Thoennes et al., 2008).

So far, two structurally unrelated classes of viral fusion proteins have been identified (class I in myxo-, paramyxo-, retro-, filo-, and coronaviruses and class II in α- and flaviviruses; Kielian and Rey, 2006), together with a third class that combines features of both class I and II (rhabdo- and herpesviruses; Weissenhorn et al., 2007; White et al., 2008). They all comprise representatives that are triggered by acidic pH. Despite the knowledge of atomic structures from all three protein classes (Weissenhorn et al., 2007; Harrison, 2008; White et al., 2008), it proved difficult, both in experimental and molecular simulation approaches, to conclusively answer the question of whether the initial trigger for destabilization and conformational changes is provided by the protonation of individual histidine residues, by combinations thereof, or by a cumulative effect through the increase of positive charge (Kampmann et al., 2006; Mueller et al., 2008; Thoennes et al., 2008). In class II fusion proteins, the molecular sensors for triggering fusion have not yet been identified. We therefore conducted a study in a prototypic class II fusion protein system (the flavivirus tick-borne encephalitis virus [TBEV]) and provide experimental evidence that the protonation of a specific histidine plays a key role for the destabilization of an intramolecular interface in the fusion protein and thus allows the initiation of the fusion process.

Flaviviruses (genus *Flavivirus* and family Flaviviridae) have an acidic pH–dependent fusion machinery (Stiasny and Heinz, 2006) and comprise several closely related important human pathogens, including yellow fever, dengue, Japanese

Correspondence to Karin Stiasny: karin.stiasny@meduniwien.ac.at

Abbreviations used in this paper: DI, domain I; FP, fusion peptide; RSP, recombinant subviral particle; sE, soluble E; TBEV, tick-borne encephalitis virus; WT, wild type.

The online version of this article contains supplemental material.

The Rockefeller University Press $30.00
J. Cell Biol. Vol. 183 No. 2 353–361
www.jcb.org/cgi/doi/10.1083/jcb.200806081

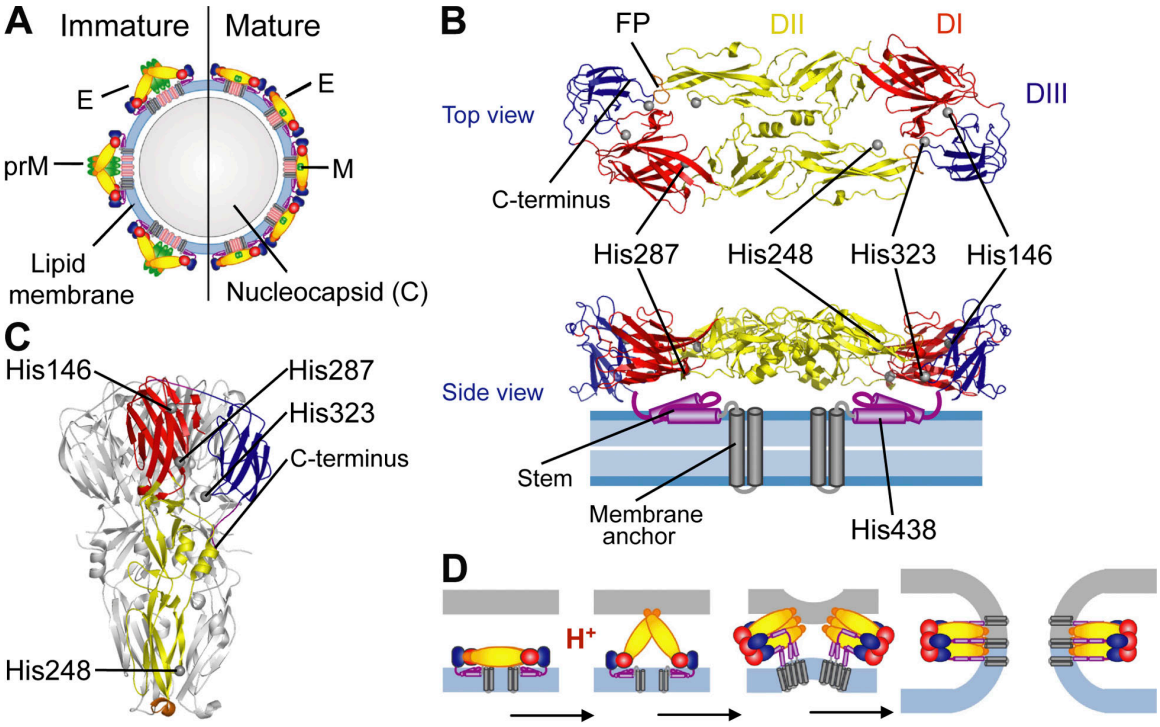

Figure 1. **Summary of the organization of flavivirus particles, the three-dimensional structures of the flavivirus envelope protein E, and a model of flavivirus membrane fusion.** (A) Schematic diagram of a flavivirus particle in its immature (prM-containing) and mature form after proteolytic cleavage of prM. (B) Schematic of the prefusion E dimer including ribbon diagrams of the TBEV sE ectodomain (top and side view) and those parts for which the atomic structure is not known (stem and anchor). (C) Ribbon diagram of the postfusion TBEV sE trimer (side view). The positions of the histidines conserved in all flavivirus E proteins are indicated by gray balls. (D) Schematic of the proposed flavivirus fusion mechanism showing different steps of the fusion process. (step 1) Metastable E dimer in mature virions. (step 2) Dissociation of the E dimers at acidic pH, outward projection of E monomers, and interaction of the FP with the target membrane. (step 3) Trimerization, DIII relocation, and "zipping up" of the stem. (step 4) Formation of the postfusion trimer and opening of the fusion pore. Red, DI; yellow, DII; blue, DIII; orange, FP; purple, stem (linker between DIII and the transmembrane anchors); gray, transmembrane anchors.

encephalitis, West Nile, and TBE viruses (Gubler et al., 2007). The surface of mature flaviviruses is made up of a herringbone-like assembly of 90 homodimers of the envelope glycoprotein E (Kuhn et al., 2002; Mukhopadhyay et al., 2003). The atomic structures of soluble forms of E (sE), lacking the membrane anchor and the so-called stem (Fig. 1 B), have been determined for different flaviviruses in pre- and postfusion conformations (Fig. 1, B and C; Rey et al., 1995; Modis et al., 2003, 2004, 2005; Bressanelli et al., 2004; Zhang et al., 2004; Kanai et al., 2006; Nybakken et al., 2006). In the prefusion conformation, the internal fusion peptide (FP) loop at the tip of domain II (DII) is buried through the interaction with a hydrophobic pocket provided by DI and III of the second partner in the homodimer (Fig. 1 B). Exposure to acidic pH leads to the initiation of the fusion process as depicted in Fig. 1 D.

Five histidine residues, located in DI, II, and III as well as in the stem region (Fig. 1, B and C), are conserved among all flavivirus E proteins and their function as pH sensors in flavivirus fusion has been discussed (Bressanelli et al., 2004; Kampmann et al., 2006; Kanai et al., 2006; Nybakken et al., 2006; Mueller et al., 2008). To support this hypothesis experimentally, we used recombinant subviral particles (RSPs) of TBEV as a model and targeted the conserved histidines in a mutational approach. As shown previously, RSPs are excellent tools for studying flavivirus fusion because they contain a lipid membrane, carry the E protein in a conformation that is indistinguishable from that on the virus, and, most importantly, display fusion characteristics similar to those of infectious virions (Schalich et al., 1996; Corver et al., 2000). This system allowed us to study the effect of histidine replacements on the different steps of fusion in the absence of resuscitating mutations that would occur during virus replication.

In our work, we demonstrate that His323, located at the interface of DI and III in the prefusion conformation of E, has a crucial function as a pH sensor for initiating fusion. Surprisingly, three of the five conserved histidines in E were shown to be completely dispensable for the early phases of fusion but two of these residues appeared to contribute to the overall stability of the postfusion trimer.

Results

Generation of RSPs with mutated His residues

The RSPs of TBEV used in this study display similar fusion characteristics as infectious virions and are assembled in eukaryotic cells after transfection with plasmids that coexpress prM and E. Their maturation and secretion pathway follows that of whole virions, including the cleavage of prM in the trans-Golgi network to yield mature and fusion-active particles (Schalich et al., 1996). To obtain specific information on the molecular pH sensors of fusion, we replaced each of the five absolutely

Table I. **WT and mutant RSPs of TBEV used in this study**

Mutant	Location of mutations
WT	–
H248N	DII
H287A	DI
H323A	DIII
H438N	stem
H248N-H287A	DII + I
H248N-H323A	DII + III
H248N-H438N	DII + stem
H287A-H438N	DI + stem
H248N-H287A-H438N	DII + I + stem

conserved histidines (and combinations thereof) in the E protein of RSPs by alanine or other amino acids and investigated their effect on fusion and fusion-related properties. Any mutation introduced into this system can potentially also interfere with processes unrelated to fusion, such as proper protein folding, oligomerization, particle formation, intracellular transport, protein processing, and maturation and secretion of RSPs. We therefore performed a meticulous analysis of the mutant RSPs to ensure that the amino acid substitutions had not influenced their wild-type (WT)–like properties at neutral pH. This was accomplished by a series of quality control measures, including an analysis of the amount of RSPs secreted from transfected cells, the sedimentation behavior in sucrose gradients, the extent of the maturation cleavage of prM, the oligomeric state of E, and the reactivity of the RSPs with a panel of 22 mAbs. These mAbs recognize epitopes in each of the three domains of the mature E protein and have proven to be excellent tools for measuring conformational differences or changes (Heinz et al., 1994; Allison et al., 1995, 2001; Stiasny et al., 2005).

To replace the histidines, we used alanine as a first choice, but, if an alanine mutation did not yield RSPs conforming to all of the criteria listed in the previous paragraph, other amino acids were substituted. Table I displays those single and combination mutants that passed all of the quality controls and were selected for the analyses described in this work. As can be seen from the table, WT-like RSPs were obtained with mutations at four of the five positions of conserved histidines, in two cases with alanine and in two cases with asparagine substitutions. The exception was His146; in this case replacement by any of the other 19 amino acids resulted in the abolition of proper RSP formation and/or secretion (Table S1, available at http://www.jcb.org/cgi/content/full/jcb.200806081/DC1).

Fusion activity of His mutant RSPs

Having certified that the replacement of histidines by other amino acids had not changed the overall conformation of E and its oligomeric state (nor did it impair particle formation, maturation, or secretion), we analyzed the effect of these mutations on fusion activity. For this purpose, the membranes of each of the mutant RSPs were fluorescence labeled in vivo with 1-pyrenehexadecanoic acid and subjected to an in vitro fusion assay (see Materials and methods). These RSPs were mixed with unlabeled liposomes and the decrease in pyrene excimer

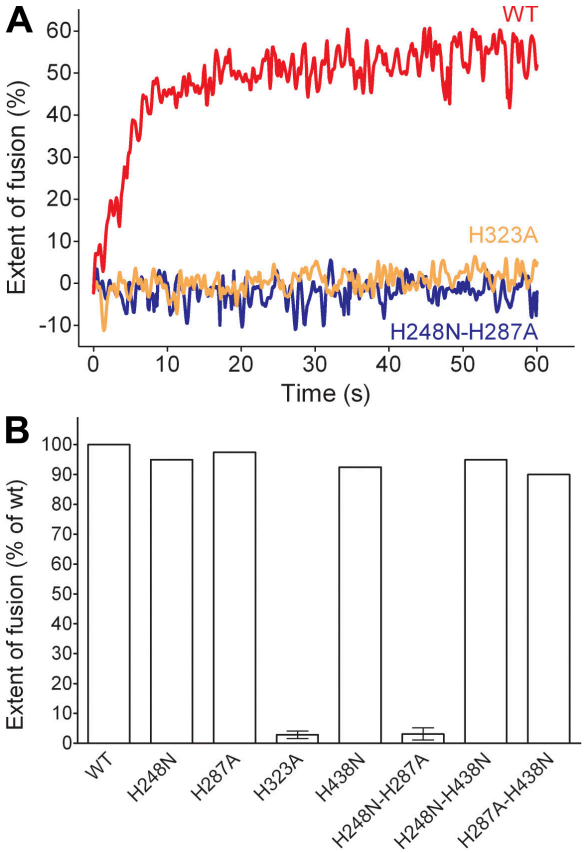

Figure 2. **Fusion activity of pyrene-labeled WT and mutant RSPs with liposomes at acidic pH.** (A) Kinetic fusion curves of RSP WT (red) and the mutant RSPs H323A (orange) and H248N-H287A (blue) at pH 5.4. (B) Extent of fusion after 60 s of mutant RSPs relative to that of the WT (set at 100%). The experiments with those mutants that were significantly different from the WT were performed at least twice and the error bars represent the standard errors of the means.

fluorescence (caused by dilution of the probe in the target membrane) was continuously monitored. Consistent with previous results (Corver et al., 2000), WT RSPs fused rapidly at pH 5.4 within the first seconds after acidification (Fig. 2 A), and the fusion activities of mutants lacking a histidine residue at position 248, 287, or 438 were identical to that of the WT (Fig. 2 B). The replacement of His323, however, resulted in the loss of fusion activity (Fig. 2, A and B), even at pH 5.0 (not depicted). We also analyzed combinations of mutations that alone did not affect fusion, i.e., H248N+H287A, H248N+H438N, and H287A+H438N. Unexpectedly, one of these combinations (H248N+H287A) impaired fusion to the same extent as did the replacement of His323 (Fig. 2, A and B). These experiments revealed the importance of individual conserved histidines for E-mediated fusion, but it remained unclear at which stage or how certain residues were involved in this multistep process.

Effect of His mutations on FP exposure

It was the primary hypothesis of our work that histidines play a role as pH sensors and that their protonation would be the initial trigger for fusion. To analyze the very first step of the fusion process, we made use of an FP-specific mAb (A1) and developed an assay that allowed us to measure the acidic pH–induced

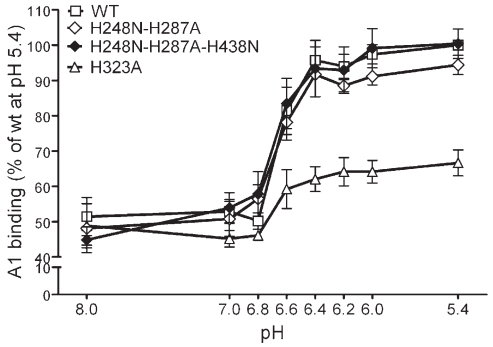

Figure 3. **Acidic pH–induced FP exposure as measured by the binding of the FP-specific mAb A1.** Results are expressed as a percentage of the maximal reactivity of A1 obtained with the WT at pH 5.4. The data are the means of three independent experiments performed in duplicate; the error bars represent the standard errors of the means.

disengagement of the FP from its protecting interactions in the E dimer and its exposure to the environment. In previous experiments, we had found that during conversion of E from the prefusion dimer to the postfusion trimer the accessibility of the FP for mAb A1 was transiently increased but lost upon conversion into the final trimeric conformation (Stiasny et al., 2007). We therefore measured this transient FP exposure using an enzyme immunoassay in which the antibody was already present in the RSP samples at the time of their acidification (see Materials and methods). The results of these experiments are shown in Fig. 3. With the exception of mutant H323A, none of the three other single His mutants differed significantly from the WT, neither with respect to the extent nor to the pH threshold of FP exposure (unpublished data). The same holds true for the double and triple mutants, which all displayed a WT-like pattern (Fig. 3). In contrast, FP exposure was severely impaired in the case of the H323A mutant, but the residual activity was induced at the same pH threshold as with the WT, i.e., around pH 6.6 (Fig. 3). These results allow us to conclude that of the four histidines analyzed only His323 plays an important role as an initial fusion trigger and that the lack of fusion activity observed with the double mutant H248N-H287A was caused by an impairment of later steps of fusion.

Loss of membrane interactions by His mutations

According to the proposed scheme of flavivirus membrane fusion (Fig. 1 D), the exposure of the FP allows its interaction with target membranes and thus mechanistically initiates the fusion process. To assess whether the observed FP exposure indeed correlated with the proposed functional activity, we performed liposome coflotation experiments for measuring membrane binding. Preparations of WT and His mutant RSPs were mixed with liposomes, acidified, and applied to sucrose step gradients as described in Materials and methods. Coflotation of E to the top of the gradients indicates either binding to or fusion with liposomes. The results of these experiments as depicted in Fig. 4 precisely matched those of the FP exposure assay (Fig. 3). With the exception of the severely impaired mutant H323A, all of the other single and combination mutants

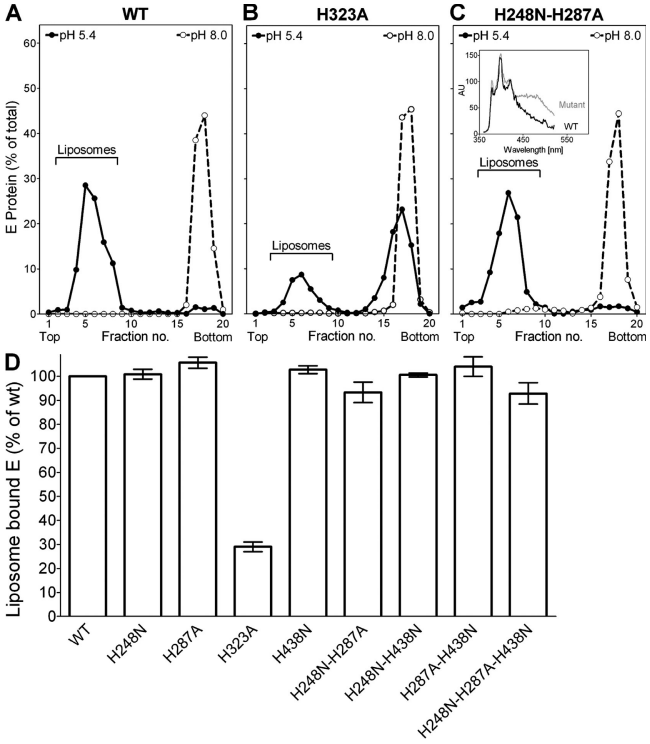

Figure 4. **Acidic pH–induced coflotation of WT and mutant RSPs with liposomes.** RSPs were incubated with liposomes at pH 5.4 (solid lines) and 8.0 (dotted lines), back-neutralized, and then subjected to centrifugation in sucrose step gradients. The gradients were fractionated, and the amount of E protein in each fraction was determined by a quantitative four-layer ELISA. The top fractions containing RSPs coflotated with the liposomes are indicated by a bracket. (A–C) Representative examples of the analysis of the step gradients obtained with WT (A) and the fusion-negative mutants H323A (B) and H248N-H287A (C). The inset in C shows the fluorescence spectrum of the coflotated fractions of the mutant (gray) relative to those of the WT (black) from experiments using pyrene-labeled RSPs. AU, arbitrary units. (D) Extent of acidic pH–induced coflotation of E with liposomes obtained with mutant RSPs relative to the WT (set at 100%). The data are the means from at least two independent experiments; the error bars represent the standard errors of the means.

displayed the same acidic pH–induced coflotation behavior as the WT. Because the double mutant H248N-H287A was completely fusion negative (Fig. 2), we made sure that its unimpaired coflotation was indeed only caused by binding to the liposomes, in the absence of fusion. For that purpose, coflotation assays were performed with pyrene-labeled samples of the mutant and WT RSPs, and fluorescence emission spectra were recorded with the coflotated fractions. In the case of RSP H248N-H287A, a strong pyrene excimer peak (which equals no dilution of the fluorescence probe) was observed, whereas it was strongly reduced with coflotated WT RSPs (Fig. 4 C, inset). These results thus allowed the unambiguous conclusion that the coflotation with the double mutant, in contrast to that of the WT, was caused by an interaction with liposomes in the absence of fusion activity.

Impairment of the formation and stability of E trimers

The results obtained so far indicated that only His323, but none of the other histidines investigated, was involved in the

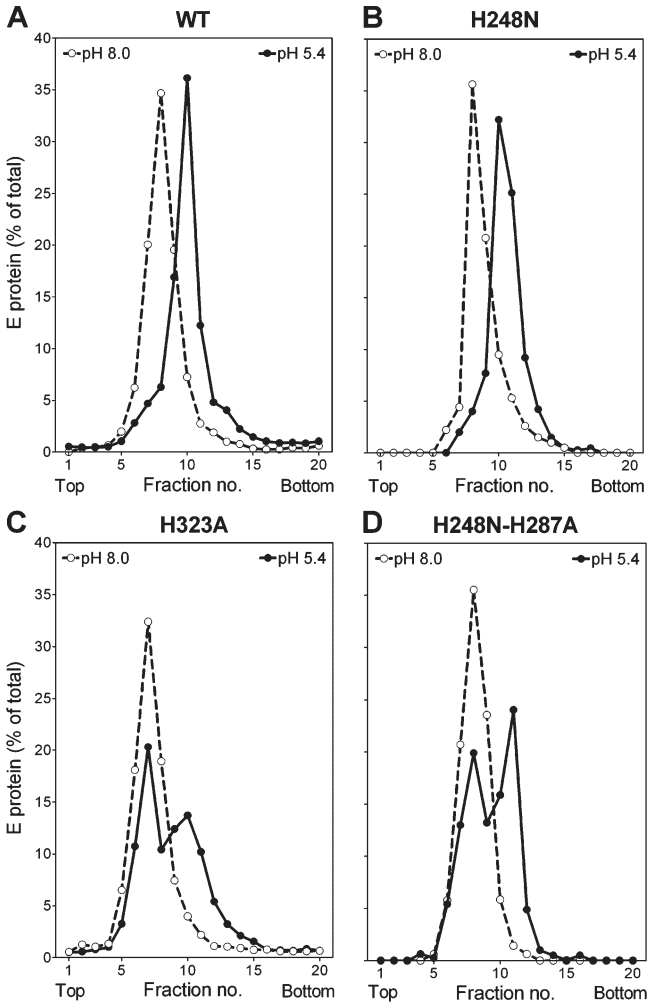

Figure 5. **Analysis of acidic pH–induced trimer formation with WT and mutant RSPs by rate zonal gradient centrifugation.** (A–D) RSPs were incubated for 10 min at pH 5.4 (solid line) or 8.0 (dotted line), back-neutralized, solubilized with 1% Triton X-100, and analyzed by sedimentation in 7–20% sucrose gradients containing 0.1% Triton X-100. The gradients were fractionated, and the amount of E protein in each fraction was determined by a quantitative four-layer ELISA. The sedimentation direction is from left to right. Peak of the E dimer, fraction 8; peak of the E trimer, fraction 10.

initiation of fusion. We therefore hypothesized that the lack of fusion observed with the double mutant H248N-H287A was caused by an impairment of later steps, such as the formation and/or stability of the E trimer. We addressed this question by sedimentation analyses and investigated the effect of each of the His mutations on the acidic pH–induced conversion of E dimers into trimers. Like with the WT RSPs, a quantitative E dimer to trimer transition was observed with the single mutants H248N, H287A, and H438N, as well as with the double mutants H248N-H438N and H287A-H438N (Fig. 5, A and B; and not depicted). In contrast, trimer formation was impaired with H323A and H248N-H287A (Fig. 5, C and D). Similar to the situation found with the pH dependence of FP exposure (Fig. 3), the pH threshold for the oligomeric rearrangement was identical to the WT with all of the mutants (pH 6.6), irrespective of the amount of trimers formed (Fig. 6).

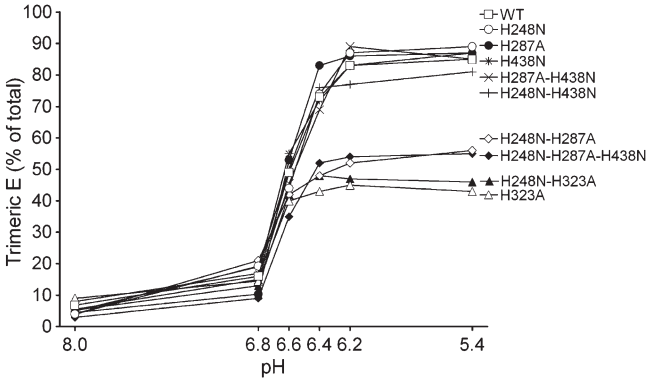

Figure 6. **pH threshold of E trimer formation of RSP WT and mutants.** Extent and pH dependence of acidic pH–induced E trimer formation with WT and mutant RSPs as determined by rate zonal sucrose density centrifugation. Results are expressed as a percentage of E found in the trimer peak fractions relative to the total amount of E in the gradient.

Because the mutations introduced into E may not only influence the formation of trimers but also their stability, we performed thermal denaturation experiments as follows. RSPs were acidified, back-neutralized, solubilized, incubated at 37 or 70°C, and subjected to rate zonal sucrose density gradient centrifugation to determine the oligomeric state of E (Fig. 7). E trimers of the single mutants H248N, H287A, and H438N were as stable as WT trimers (Fig. 7 and not depicted). In contrast, not only was trimer formation with H323A and H248N-287A less efficient (Fig. 5, C and D) but also these trimers were sensitive to incubation at 70°C, as revealed by a strong reduction of the E trimer peak and an accumulation of presumably denatured and aggregated material in the pellet (Fig. 7). As expected, similar results were obtained when trimer formation was allowed to proceed in the presence of liposomes (unpublished data).

Collectively, these results allow two important conclusions: (1) the lack of fusion activity of mutant H248N-H287A is likely to be caused by an impairment of trimer formation combined with a reduction in trimer stability, and (2) H323 apparently has a double role in the fusion process and not only functions as a pH sensor for initiating fusion but also contributes to the stability of the postfusion trimer.

Discussion

Although histidines have been speculated to play an important role as acidic pH sensors in class II viral fusion proteins (Bressanelli et al., 2004; Kampmann et al., 2006; Kanai et al., 2006; Nybakken et al., 2006; Roussel et al., 2006; Mueller et al., 2008), experimental evidence for such a role is still lacking. The mutational analysis presented in this work suggests that one of the five conserved histidines in the TBEV E protein (His323) plays a dominant role in the initiation of the multistep fusion process. This amino acid residue forms part of an intricate intramolecular network of interactions between DI and III of the E monomer in its prefusion conformation, consisting of hydrogen bonds, van der Waals contacts, and a salt bridge between Arg9 in DI and Glu373 in DIII (Fig. 8 A; Bressanelli et al., 2004). Both of these amino acids as well as several additional residues of this contact

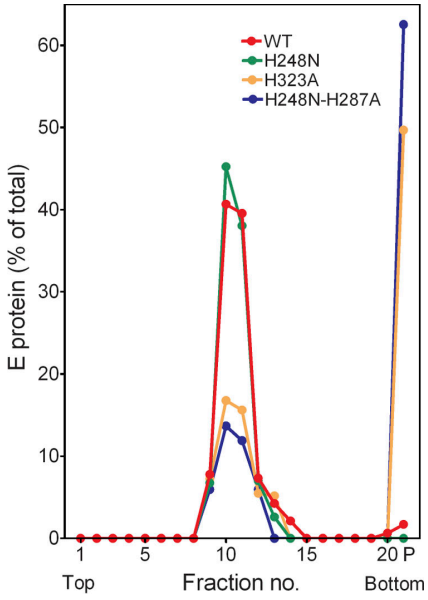

Figure 7. **Analysis of the stability of acidic pH–induced E trimers of WT and selected mutant RSPs.** Acidic pH–induced trimers of WT (red) and mutant RSPs (green, H248A; orange, H323A; blue, H248A-H287N) were exposed to 70°C and subjected to rate zonal sucrose density gradient centrifugation. The sedimentation direction is from left to right. The pellet (P) was resuspended in 0.6 ml corresponding to the volume of a single fraction.

area are absolutely conserved among flaviviruses (Bressanelli et al., 2004). The integrity of this domain interface is essential for the dimeric conformation of E in mature virions because only in this specific arrangement do the two domains together provide a protective pocket for the FP loop at the tip of DII of the second subunit (Fig. 1 B and Fig. 8 A). Through these and other DII interactions, the monomeric subunits are fixed in an antiparallel orientation in the E dimer. The release of these constraints is necessary for exposing the FP and allowing an outward projection of the E monomers as a prerequisite for target membrane interactions (Mukhopadhyay et al., 2005; Stiasny and Heinz, 2006; Harrison, 2008). Inspection of the postfusion structure suggests that His323 may form an intradomain salt bridge with Glu373. Because in the prefusion conformation Glu373 is part of the central salt bridge together with Arg9, the protonation of His323 is likely to contribute to the dissolution of this salt bridge and to the concomitant destabilization of the DI–DIII interface. The fact that the basic architecture of these networks is conserved in the pre- and postfusion forms of E from TBEV and the distantly related dengue 2 virus (His323 and His317 and Glu373 and Glu368, respectively) would argue for a similar mechanism of fusion initiation in all flaviviruses (Rey et al., 1995; Bressanelli et al., 2004; Modis et al., 2003, 2004).

The DI–DIII interface contains another absolutely conserved histidine at position 146 (Fig. 8 A), which we were not able to investigate directly because its replacement by any of the other 19 amino acids abolished the formation of native RSPs by the quality criteria applied. Although the mutation H323A dramatically reduced the acidic pH–induced exposure of the FP, there was some residual activity that occurred at the same pH threshold of 6.6. Because all of the other His mutations as well as their combinations did not impair FP exposure, the residual activity is probably related to the protonation of His146 and suggests a possible accessory role of this residue in the destabilization of the DI–DIII interface. Surprisingly, and in contrast to what has been observed for the influenza virus class I fusion protein hemagglutinin (Thoennes et al., 2008), none of the histidine mutations in this work affected the pH threshold of fusion-related processes. Flavivirus variants that exhibited a pH shift for membrane fusion were described to contain mutations in the DI–DII hinge region (Rey et al., 1995; Harrison, 2008), but the mechanism causing this behavior remains to be elucidated. It has been suggested, however, that these mutations influence the stability of E (Modis et al., 2003) and thus may modulate the pH required to induce those conformational changes that drive fusion. Such "stability effects," however, appear to be distinct from the actual pH-sensoring machinery, which apparently involves His323 and probably His146.

The conversion of the E dimer to the postfusion trimer not only requires the relocation of DIII but also a change in the orientation of DII relative to DI (Bressanelli et al., 2004; Modis et al., 2004). This is made possible by the structural flexibility of the junction between the two domains (Modis et al., 2003), which is also necessary for conformational transitions during other phases of the viral life cycle, such as virus assembly and maturation (Zhang et al., 2004; Li et al., 2008). In the context of fusion, this hinge motion may occur spontaneously upon release from dimer constraints, caused by the dissolution of the DI–DIII interface, but could also require an independent pH-sensoring step (Kanai et al., 2006). With respect to the conserved histidine at the DI–DII junction (His287), we did not, however, find evidence for such a pH sensor function because its replacement did not have any measureable effect, neither on early nor late stages of fusion.

It is a further finding of our work that His323 apparently has a dual role in the fusion process and contributes both to the initial pH trigger and to the stability of the postfusion trimer. The lower stability of this mutant trimer could be a result of the lack of the salt bridge between His323 and Glu373 in the postfusion structure of DIII (Fig. 8 B) and a concomitant weakening of DIII-mediated trimer contacts and/or the proper positioning of the stem for zippering along the grooves provided by DII. None of the other conserved histidines (except His146, which was irreplaceable and therefore not amenable to analysis) seems to have a similar impact on E trimerization as His323 because their single replacements neither affected trimer formation nor trimer stability to a measurable extent (Fig. 7). An additive effect, however, was observed in the double mutant H248N-H287A, which was fusion negative and was impaired in trimer formation and trimer stability as was the mutant H323A. His287 forms part of the trimer interfaces (Fig. 1 C) and His248 is located at a position at the groove, close to the FP (Fig. 1 C), that is likely to accommodate the stem during the "zipping up" process (Fig. 1 D). Theoretically, the replacement of each of these residues alone could interfere with late stages of the fusion process, leading to the opening of the fusion pore. More specific interpretations of these results, however, will depend on the elucidation of the atomic structure of the stem in the postfusion structure of E and assays that distinguish between lipid and contents mixing.

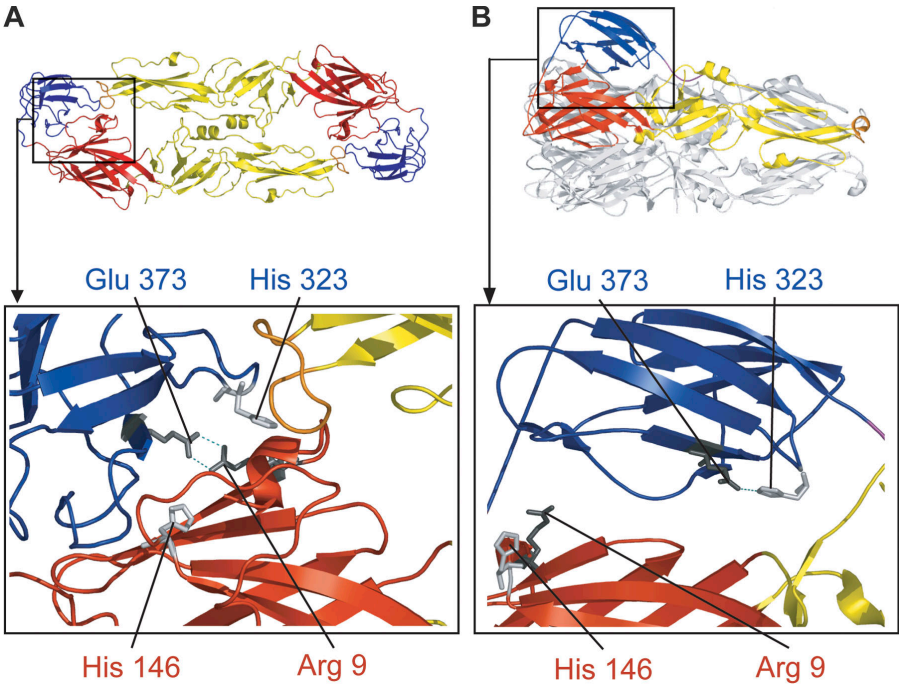

Figure 8. **Intramolecular interactions of DIII in the pre- and postfusion structures of sE.** (A) Ribbon diagrams of the TBEV sE dimer and the details of the DI–DIII interface in the prefusion conformation with the central salt bridge between Arg9 and Glu373. (B) Ribbon diagrams of the TBEV sE trimer and the details of DIII in its postfusion conformation revealing the possible salt bridge between His323 and Glu373.

Although three of the conserved histidines in TBEV E (His248, His287, and His438) were ruled out as pH sensors for initiating fusion, they could be involved in other pH-dependent mechanisms, such as the conversion of immature (containing prM-E) into mature particles (Yu et al., 2008). The structure of the prM-E heterodimer of dengue 2 virus has recently been determined by x-ray crystallography and it is of special interest that His244 (corresponding to His248 in TBEV-E) is situated opposite a conserved Asp63 in prM (Li et al., 2008). It has therefore been speculated that the loss of protonation of His244 could be required for the release of the pr-peptide at neutral pH (Li et al., 2008; Yu et al., 2008). In our TBEV system, the replacement of the homologous His248, however, had no apparent effect on virus maturation and further experiments will be necessary to clarify this issue.

Despite the structural similarity of the class II fusion proteins of alphaviruses (E1) and flaviviruses (E; Kielian, 2006), it is likely that the pH-sensoring machineries for initiating fusion are significantly different in the two virus systems. Indeed, there is only one conserved histidine at a strictly homologous position in E and E1. This residue (His248 in TBEV and His230 in Semliki Forest virus, respectively), however, has been ruled out as a pH sensor for both viruses and was shown to affect only a late stage of fusion (Chanel-Vos and Kielian, 2004, 2006; this study). The major difference lies in the structural details of FP protection in the prefusion conformations of E and E1. In flaviviruses, the FP in E is buried through homodimeric interactions, whereas in alphaviruses, the FP in E1 is protected by a heterodimeric interaction with a second, overlying protein (E2; Kielian, 2006). Alphavirus fusion could therefore be triggered by the protonation of as yet unidentified residues in both E1 and E2.

In conclusion, our study provides experimental information on the pH trigger of flavivirus membrane fusion and the critical role of the DI–DIII interface in this process. Although several of the absolutely conserved histidines in the viral fusion protein were shown to be completely dispensable for fusion initiation, our study does not rule out possible roles of these residues in other pH-dependent processes of the viral life cycle. These new insights can also contribute to the design of antiviral approaches that target the structural transitions of flaviviruses during entry and morphogenesis.

Materials and methods

Mutagenesis of RSPs

Using the site-directed mutagenesis kit Gene Tailor (Invitrogen), mutations were introduced into the recombinant plasmid SV-PE WT (Allison et al., 1994), which contained the TBEV prM and E genes under the control of an SV40 early promoter, at the codon positions 146, 248, 287, 323, and 438 of the E gene. The WT and mutant plasmids were sequenced throughout the prM and E regions to confirm that only the desired mutations were present.

Production of RSPs

For the production of RSPs, COS-1 cells were transfected with recombinant plasmids by electroporation as described previously (Schalich et al., 1996). RSPs were harvested 48 h after transfection from cell culture supernatants, pelleted by ultracentrifugation, and purified by sucrose gradient centrifugation (Schalich et al., 1996; Allison et al., 2001). For membrane fusion (lipid mixing) assays, the RSPs were metabolically labeled with 1-pyrenehexadecanoic acid (Invitrogen) as described previously (Corver et al., 2000; Allison et al., 2001).

Quality controls of RSPs

The amount of RSPs secreted from transfected cells was quantified by a four-layer ELISA after solubilization with 0.4% sodium dodecyl sulfate at 65°C for 30 min (Heinz et al., 1994). The conformation of E was probed in comparison to that of the WT by epitope mapping with 22 E protein–specific mAbs (Allison et al., 1995, 2001; Heinz et al., 1994; Stiasny et al., 2005) and their maturation state (presence of prM) was analyzed by Western blotting (Allison et al., 2003).

pH treatment of RSPs

Acidic pH incubations were performed at 37°C and the different acidic pHs were adjusted by the addition of morpholinoethansulfonic acid (MES)

ranging from 80 to 300 mM to the samples in TAN buffer, pH 8.0 (50 mM triethanolamine and 100 mM NaCl). Controls were incubated in TAN buffer, pH 8.0.

Lipid mixing fusion assay

Pyrene-labeled RSPs were mixed with large unilamellar liposomes (0.3-mM total lipid) consisting of phosphatidylcholine, phosphatidylethanolamine, and cholesterol (molar ratio 1:1:2) in a continuously stirred fluorimeter cuvette at 37°C (Allison et al., 2001; Stiasny et al., 2003). Fluorescence was monitored continuously using a fluorescence spectrophotometer (LS-50B; Perkin-Elmer). Lipid mixing was initiated by the addition of MES to yield a final pH of 5.4. The extent of fusion was calculated by using the initial excimer fluorescence as 0% fusion and the fluorescence after solubilization of the RSP-liposome mixture by the detergent octa(ethylene glycol)-*n*-dodecyl monoether (Sigma-Aldrich) as 100% fusion.

Coflotation assay

Purified RSPs were mixed with liposomes with the same composition as those used in the fusion assays at a ratio of 1 µg of E protein to 200 nmol of lipids. The mixture was acidified by the addition of MES to yield a pH of 5.4 and incubated for 15 min at 37°C. After back-neutralization by the addition of 150 mM triethanolamine to yield a final pH of 7.8, sucrose was added to the RSP-liposome mixture to a final concentration of 20% (wt/wt). This 0.6-ml sample was layered onto a 1-ml cushion of 50% sucrose in TAN buffer, pH 8.0, and overlaid with 1.4 ml of 15% sucrose and 1 ml of 5% sucrose (Allison et al., 2001; Stiasny et al., 2002). The step gradients were centrifuged for 2 h at 4°C (rotor SW 55; Beckman Coulter) at 50,000 rpm, and 0.2-ml fractions were collected by upward displacement using a Piston Gradient Fractionator (BioComp Instruments Inc.). E protein was quantified by four-layer ELISA after solubilization with 0.4% sodium dodecyl sulfate at 65°C for 30 min (Heinz et al., 1994).

FP exposure assay

Native RSPs (at a concentration of 0.5 µg/ml of E protein) in phosphate-buffered saline, pH 7.4, containing 2% lamb serum were captured by polyclonal anti-TBEV immunoglobulin G for 1 h at 37°C as described previously (Stiasny et al., 2007). The exposure of the FP was measured by the addition of biotinylated mAb A1 (FP-specific mAb) in MES buffer (50 mM MES and 100 mM NaCl), titrated to the appropriate pH by titration with 1 N NaOH. After incubation for 1 h at 37°C, the bound antibody A1 was detected by using streptavidin-peroxidase (Sigma-Aldrich).

E trimer formation and stability

The acidic pH–induced E dimer-to-trimer transition was measured by sedimentation analysis as described previously (Allison et al., 1995, 2001). 3 µg RSPs in TAN buffer, pH 8.0, were adjusted to different acidic pHs by the addition of MES (see pH treatment of RSPs) and incubated at 37°C for 10 min. Samples were back-neutralized with 150 mM triethanolamine, solubilized for 1 h at room temperature with 1% Triton X-100, and applied to 7–20% (wt/wt) continuous sucrose gradients containing 0.1% Triton X-100. Centrifugation was performed for 20 h at 38,000 rpm at 15°C (rotor SW 40; Beckman Coulter). 0.6-ml fractions were collected by upward displacement using a Piston Gradient Fractionator, and the amount of E in each fraction was determined by an E-specific four-layer ELISA after treatment with 0.4% sodium dodecyl sulfate at 65°C for 30 min (Heinz et al., 1994). To investigate the thermostability of the postfusion E protein, acidic pH–pretreated and solubilized RSPs were incubated at 37 and 70°C before sedimentation analysis (Stiasny et al., 2005).

Online supplemental material

Table S1 lists all of the additional histidine mutants that were generated in the course of this project and, in contrast to the mutants in Table I, did not lead to the secretion of particles into the transfected cell culture supernatants. Online supplemental material is available at http://www.jcb.org/cgi/content/full/jcb.200806081/DC1.

We thank Gabriel O'Riordain and Christian Taucher for critical reading of the manuscript.

This work was supported by the Austrian Science Fund (P19843-B13).

The authors declare that they have no competing financial interests.

Submitted: 13 June 2008
Accepted: 27 August 2008

References

Allison, S.L., C.W. Mandl, C. Kunz, and F.X. Heinz. 1994. Expression of cloned envelope protein genes from the flavivirus tick-borne encephalitis virus in mammalian cells and random mutagenesis by PCR. *Virus Genes.* 8:187–198.

Allison, S.L., J. Schalich, K. Stiasny, C.W. Mandl, C. Kunz, and F.X. Heinz. 1995. Oligomeric rearrangement of tick-borne encephalitis virus envelope proteins induced by an acidic pH. *J. Virol.* 69:695–700.

Allison, S.L., J. Schalich, K. Stiasny, C.W. Mandl, and F.X. Heinz. 2001. Mutational evidence for an internal fusion peptide in flavivirus envelope protein E. *J. Virol.* 75:4268–4275.

Allison, S.L., Y.J. Tao, G. O'Riordain, C.W. Mandl, S.C. Harrison, and F.X. Heinz. 2003. Two distinct size classes of immature and mature subviral particles from tick-borne encephalitis virus. *J. Virol.* 77:11357–11366.

Bressanelli, S., K. Stiasny, S.L. Allison, E.A. Stura, S. Duquerroy, J. Lescar, F.X. Heinz, and F.A. Rey. 2004. Structure of a flavivirus envelope glycoprotein in its low-pH-induced membrane fusion conformation. *EMBO J.* 23:728–738.

Carneiro, F.A., F. Stauffer, C.S. Lima, M.A. Juliano, L. Juliano, and A.T. Da Poian. 2003. Membrane fusion induced by vesicular stomatitis virus depends on histidine protonation. *J. Biol. Chem.* 278:13789–13794.

Chanel-Vos, C., and M. Kielian. 2004. A conserved histidine in the ij loop of the Semliki Forest virus E1 protein plays an important role in membrane fusion. *J. Virol.* 78:13543–13552.

Chanel-Vos, C., and M. Kielian. 2006. Second-site revertants of a Semliki Forest virus fusion-block mutation reveal the dynamics of a class II membrane fusion protein. *J. Virol.* 80:6115–6122.

Corver, J., A. Ortiz, S.L. Allison, J. Schalich, F.X. Heinz, and J. Wilschut. 2000. Membrane fusion activity of tick-borne encephalitis virus and recombinant subviral particles in a liposomal model system. *Virology.* 269:37–46.

Gubler, D., G. Kuno, and L. Markhoff. 2007. Flaviviruses. *In* Fields Virology. D.M. Knipe, P.M. Howley, D.E. Griffin, R.A. Lamb, M.A. Martin, B. Roizman, and S.E. Straus, editors. Lippincott Williams & Wilkins, Philadelphia. 1153–1252.

Harrison, S.C. 2008. Viral membrane fusion. *Nat. Struct. Mol. Biol.* 15:690–698.

Heinz, F.X., K. Stiasny, G. Puschner-Auer, H. Holzmann, S.L. Allison, C.W. Mandl, and C. Kunz. 1994. Structural changes and functional control of the tick-borne encephalitis virus glycoprotein E by the heterodimeric association with protein prM. *Virology.* 198:109–117.

Kampmann, T., D.S. Mueller, A.E. Mark, P.R. Young, and B. Kobe. 2006. The role of histidine residues in low-pH-mediated viral membrane fusion. *Structure.* 14:1481–1487.

Kanai, R., K. Kar, K. Anthony, L.H. Gould, M. Ledizet, E. Fikrig, W.A. Marasco, R.A. Koski, and Y. Modis. 2006. Crystal structure of West Nile virus envelope glycoprotein reveals viral surface epitopes. *J. Virol.* 80:11000–11008.

Kielian, M. 2006. Class II virus membrane fusion proteins. *Virology.* 344:38–47.

Kielian, M., and F.A. Rey. 2006. Virus membrane-fusion proteins: more than one way to make a hairpin. *Nat. Rev. Microbiol.* 4:67–76.

Kuhn, R.J., W. Zhang, M.G. Rossmann, S.V. Pletnev, J. Corver, E. Lenches, C.T. Jones, S. Mukhopadhyay, P.R. Chipman, E.G. Strauss, et al. 2002. Structure of dengue virus: implications for flavivirus organization, maturation, and fusion. *Cell.* 108:717–725.

Li, L., S.M. Lok, I.M. Yu, Y. Zhang, R.J. Kuhn, J. Chen, and M.G. Rossmann. 2008. The flavivirus precursor membrane-envelope protein complex: structure and maturation. *Science.* 319:1830–1834.

Modis, Y., S. Ogata, D. Clements, and S.C. Harrison. 2003. A ligand-binding pocket in the dengue virus envelope glycoprotein. *Proc. Natl. Acad. Sci. USA.* 100:6986–6991.

Modis, Y., S. Ogata, D. Clements, and S.C. Harrison. 2004. Structure of the dengue virus envelope protein after membrane fusion. *Nature.* 427:313–319.

Modis, Y., S. Ogata, D. Clements, and S.C. Harrison. 2005. Variable surface epitopes in the crystal structure of dengue virus type 3 envelope glycoprotein. *J. Virol.* 79:1223–1231.

Mueller, D.S., T. Kampmann, R. Yennamalli, P.R. Young, B. Kobe, and A.E. Mark. 2008. Histidine protonation and the activation of viral fusion proteins. *Biochem. Soc. Trans.* 36:43–45.

Mukhopadhyay, S., B.S. Kim, P.R. Chipman, M.G. Rossmann, and R.J. Kuhn. 2003. Structure of West Nile virus. *Science.* 302:248.

Mukhopadhyay, S., R.J. Kuhn, and M.G. Rossmann. 2005. A structural perspective of the flavivirus life cycle. *Nat. Rev. Microbiol.* 3:13–22.

Nybakken, G.E., C.A. Nelson, B.R. Chen, M.S. Diamond, and D.H. Fremont. 2006. Crystal structure of the West Nile virus envelope glycoprotein. *J. Virol.* 80:11467–11474.

Rey, F.A., F.X. Heinz, C. Mandl, C. Kunz, and S.C. Harrison. 1995. The envelope glycoprotein from tick-borne encephalitis virus at 2 A resolution. *Nature.* 375:291–298.

Roche, S., A.A. Albertini, J. Lepault, S. Bressanelli, and Y. Gaudin. 2008. Structures of vesicular stomatitis virus glycoprotein: membrane fusion revisited. *Cell. Mol. Life Sci.* 65:1716–1728.

Roussel, A., J. Lescar, M.C. Vaney, G. Wengler, G. Wengler, and F.A. Rey. 2006. Structure and interactions at the viral surface of the envelope protein E1 of semliki forest virus. *Structure.* 14:75–86.

Schalich, J., S.L. Allison, K. Stiasny, C.W. Mandl, C. Kunz, and F.X. Heinz. 1996. Recombinant subviral particles from tick-borne encephalitis virus are fusogenic and provide a model system for studying flavivirus envelope glycoprotein functions. *J. Virol.* 70:4549–4557.

Srivastava, J., D.L. Barber, and M.P. Jacobson. 2007. Intracellular pH sensors: design principles and functional significance. *Physiology (Bethesda).* 22:30–39.

Stevens, J., A.L. Corper, C.F. Basler, J.K. Taubenberger, P. Palese, and I.A. Wilson. 2004. Structure of the uncleaved human H1 hemagglutinin from the extinct 1918 influenza virus. *Science.* 303:1866–1870.

Stiasny, K., and F.X. Heinz. 2006. Flavivirus membrane fusion. *J. Gen. Virol.* 87:2755–2766.

Stiasny, K., S.L. Allison, J. Schalich, and F.X. Heinz. 2002. Membrane interactions of the tick-borne encephalitis virus fusion protein E at low pH. *J. Virol.* 76:3784–3790.

Stiasny, K., C. Koessl, and F.X. Heinz. 2003. Involvement of lipids in different steps of the flavivirus fusion mechanism. *J. Virol.* 77:7856–7862.

Stiasny, K., C. Kossl, and F.X. Heinz. 2005. Differences in the postfusion conformations of full-length and truncated class II fusion protein E of tick-borne encephalitis virus. *J. Virol.* 79:6511–6515.

Stiasny, K., S. Brandler, C. Kossl, and F.X. Heinz. 2007. Probing the flavivirus membrane fusion mechanism by using monoclonal antibodies. *J. Virol.* 81:11526–11531.

Thoennes, S., Z.-N. Li, B.-J. Lee, W.A. Langley, J.J. Skehel, R.J. Russell, and D.A. Steinhauer. 2008. Analysis of residues near the fusion peptide in the influenza hemagglutinin structure for roles in triggering membrane fusion. *Virology.* 370:403–414.

Weissenhorn, W., A. Hinz, and Y. Gaudin. 2007. Virus membrane fusion. *FEBS Lett.* 581:2150–2155.

White, J.M., S.E. Delos, M. Brecher, and K. Schornberg. 2008. Structures and mechanisms of viral membrane fusion proteins: multiple variations on a common theme. *Crit. Rev. Biochem. Mol. Biol.* 43:189–219.

Yu, I.M., W. Zhang, H.A. Holdaway, L. Li, V.A. Kostyuchenko, P.R. Chipman, R.J. Kuhn, M.G. Rossmann, and J. Chen. 2008. Structure of the immature dengue virus at low pH primes proteolytic maturation. *Science.* 319:1834–1837.

Zhang, Y., W. Zhang, S. Ogata, D. Clements, J.H. Strauss, T.S. Baker, R.J. Kuhn, and M.G. Rossmann. 2004. Conformational changes of the flavivirus E glycoprotein. *Structure.* 12:1607–1618.